Investigation of a Relativistic Cherenkov Microwave Oscillator without a Guiding Magnetic Field

E. M. Totmeninov, A.I. Klimov, S. D. Korovin, V.V. Rostov

Institute of High Current Electronics SB RAS, 2/3 Akademichesky Ave., Tomsk, 634055, Russia
ph. +7(3822)491–641, fax +7(3822)492–410, e-mail totm@lfe.hcei.tsc.ru

Conditions which ensure efficient Cherenkov radiation without external magnetic field have been considered. An analytical estimate of the path length of a continuous cylindrical electron beam in a drift tube has been made in the paraxial approximation. The influence of the electron beam premodulation on the starting current and linear efficiency of the oscillator has been analyzed. Calculations have been performed for the geometry of a relativistic Cherenkov microwave oscillator with an efficiency ≈ 30% in which a continuous cylindrical electron beam travels through a short resonance slow-wave structure ($L \approx 3\lambda$ where λ is the wavelength) in the absence of an external magnetic field. In experiments, the power of the high-current electron beam has been converted to the electromagnetic wave E_{01} with an efficiency of ~ 8% (of the total vacuum diode current) at a power of 1.2 ± 0.3 GW and at an oscillation frequency of 4.06 GHz.

1. Introduction

The currently available versions of relativistic microwave oscillators without external guiding magnetic field (e.g., vircator, MILO [1], [2]) ensure a relatively lower (~5%) efficiency of power conversion of a relativistic electron beam (REB) to electromagnetic radiation. The possible way of increasing the conversion efficiency is either to improve the available devices or to try alternative approaches to attack this problem. One such method can be based on the effect of long-term interaction of an electron beam with an electromagnetic wave in the mode of Cherenkov synchronism [3] $V_{e,0} \approx V_{ph}$ ($V_{e,0}$ is the initial longitudinal velocity of the electron beam and V_{ph} is the phase velocity of the synchronous wave or its space harmonic). The use of this mode in oscillators with an external guiding magnetic field provides sufficiently high efficiency of energy exchange. However, for efficient conversion without external guiding magnetic field, it is necessary, among other things, to solve the problems of REB transport along the interaction space and provide efficient interaction of the REB with a synchronous electromagnetic wave.

2. Estimation of the path length of a continuous cylindrical electron beam

Transportation of a continuous cylindrical REB in a drift tube can be realized at the expense of the azimuthal component of the self-magnetic field, which precludes its rapid divergence under the action of the space charge. Assume that R_A is the drift tube radius, R_b is the external beam radius, J_b is the beam current, $\beta_{//} = \sqrt{1-\gamma^{-2}}$ is the normalized longitudinal electron velocity, $\gamma = \gamma_0 - 2J_b/(J_A\beta_{//,0})\ln(R_A/R_b)$ is the relativistic gamma factor for a peripheral electron ($r = R_b$) with account of the potential sag, γ_0 is the initial electron energy, z is the longitudinal coordinate, and $J_A = mc^3/e$ is the Alfven current. At the point z=0, a transparent foil is placed through which the beam is injected into the drift tube. The beam is taken as monoenergetic with a uniform charge distribution over the beam cross-section. Using the method of electrical images [4] and the expression for the azimuthal self-magnetic field of a continuous cylindrical beam $H_\varphi = 2J_b/cR_b$, where c is the velocity of light and e is the charge of an electron, we can obtain the estimate of the beam path length L_{TR} in the paraxial approximation:

$$R_A - R_b = \frac{J_b R_b}{J_A \gamma \beta_{//}^3}\left[\ln\left(\frac{\dfrac{L_{TR}}{R_b}+\sqrt{1+\left(\dfrac{L_{TR}}{R_b}\right)^2}}{\dfrac{L_{TR}}{R_A}+\sqrt{1+\left(\dfrac{L_{TR}}{R_A}\right)^2}}\right) - \left(2-\frac{R_b}{R_A}\right)\frac{L_{TR}}{R_b} - \beta_{//}{}^2\frac{L_{TR}^2}{R_b^2} + \frac{L_{TR}}{R_b}\sqrt{1+\left(\frac{L_{TR}}{R_b}\right)^2}\right] \quad (1)$$

The results of calculations in accord with (1) are presented in Fig. 1.

As can be seen from the plots, a large discrepancy between the estimates of the path length and its values calculated with the code KARAT is found with increasing beam current and diameter ($R_b \approx R_A$), when the use of the paraxial approximation and the assumption of the monoenergetic beam in deducing (1) appear not to be quite correct.

Moreover, it follows from the numerical simulation, as opposed to (1), that for the specified beam parameters there exists an optimal value of $R_{b,opt}$ ($R_{b,opt}< R_A$) at which the largest path length is achieved in each case. Nevertheless, the obtained results, as a whole, demonstrate the possibility of transporting a continuous cylindrical REB without external guiding magnetic field for distances much larger than the drift tube diameter. In a particular case, $L_{TR}>>R_b$, R_A and $R_b=R_A$, from (1) it follows that $L_{TR} \approx R_b\gamma^2 = R_A\gamma^2$.

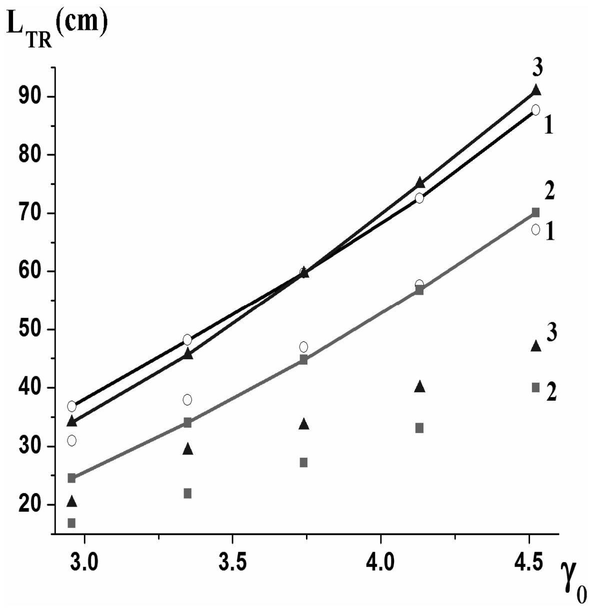

Fig. 1. Beam path length versus the initial energy. The dependences were obtained from estimation formula (1) and from numerical simulation with the code KARAT [5] (separate points) at R_A = 5 cm and $\gamma_0 \approx 3$ for: 1 – R_b = 3 cm, J_b = 5 kA, 2 – R_b = 3 cm, J_b = 10 kA, 3 – R_b = 4 cm, J_b = 10 kA.

2. Peculiarity of electron beam interaction with an electromagnetic wave

It was shown earlier [6] that with energy modulation of the electron beam at the input of a relativistic Cherenkov oscillator, synchronism detuning approaches zero when the central electron of the formed bunch at the beginning of the interaction space occurs in the decelerating phase of the synchronous harmonic field near the boundary with the accelerating filed phase (modulation phase $\approx \pi$). As the modulation depth is increased, the detuning takes on negative values. With a fixed structure of the field, we can write an expression for the active component of the electron beam susceptibility [7] which, in the presence of particle premodulation at the input, has the form:

$$-\varphi'(\upsilon_{kin}) = \frac{2(2(1-\cos(\upsilon_{kin})) - \sin(\upsilon_{kin})\upsilon_{kin})}{\upsilon_{kin}{}^3} - \frac{2|\alpha|}{\upsilon_{kin}}\left(\cos(\phi+\upsilon_{kin}) + \frac{\sin\phi}{\upsilon_{kin}} - \frac{\sin(\phi+\upsilon_{kin})}{\upsilon_{kin}}\right)$$

where $\upsilon_{kin} = \delta_0\xi_k$ is the kinematic transit angle, $\xi_k = kL$, L is the length of the interaction space, $\delta_0 = (1/V_{ph} - 1/V_{e,0})c$ is the kinematic synchronism detuning, and ϕ is the modulation phase. For $\phi \approx \pi$, an increase in premodulation depth causes the first positive maximum ($-\varphi'$) to shift toward the range of negative values of the kinematic transit angle υ_{kin}, when the phase velocity of the synchronous wave is higher than the electron velocity $V_{ph} > V_{e,0}$ (Fig. 2). To the maximum ($-\varphi'$) there corresponds $|\upsilon_{kin,opt}| \approx (0.1 \div 0.2)\pi$, which is near-invariant with further increasing modulation depth. Slowing down the traveling wave to $V_{ph} \approx c$, when the distribution of the longitudinal electric field component over the system cross-section is near-uniform for its first harmonic, ($E_z(r) \sim \exp(kcr\sqrt{V_{ph}^{-2} - c^{-2}})$), provides the condition for its efficient interaction with the continuous cylindrical REB. It is advantageous here to use a corrugated waveguide as the slow-wave structure (SWS).

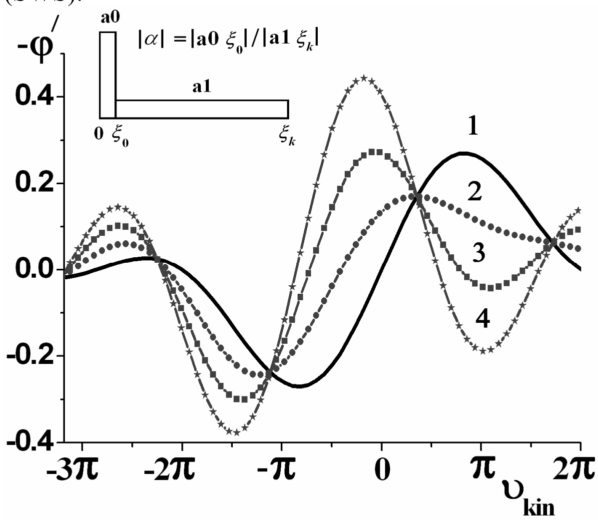

Fig. 2. Reduced active components of the electron flow susceptibility as a function of the kinematic transit angle for a fixed two-stage (narrow modulation gap at the system entrance $\xi_0 << \xi_k$) longitudinal structure of the field. The phase difference of the field in the modulator and at the entrance to the second section $\approx \pi$: 1 – $|\alpha| = 0$, 2 – $|\alpha| = 0.2$, 3 – $|\alpha| = 0.4$; 4 – $|\alpha| = 0.6$.

In this case, the presence of distributed reflections in the SWS in proximity to the π-type mode ($V_{ph} \approx c$) ensures the required internal feedback in the oscillator. Thus, the possibility exists to realize the mode with low starting current of the oscillator and with a high efficiency of energy exchange (the linear efficiency is proportional to $(-\varphi^{/}(\upsilon_{kin}))$ [7]) in the absence of an external guiding magnetic field.

3. Numerical experiment

The oscillator comprises a cathode (C), a grid anode (G), a smooth waveguide section and an SWS (Fig. 3). In the geometry in question, the average corrugation diameter is approximately 1.3 times larger than the radiation wavelength. A relativistic electron beam is injected from the planar diode to the interaction space through the anode grid.

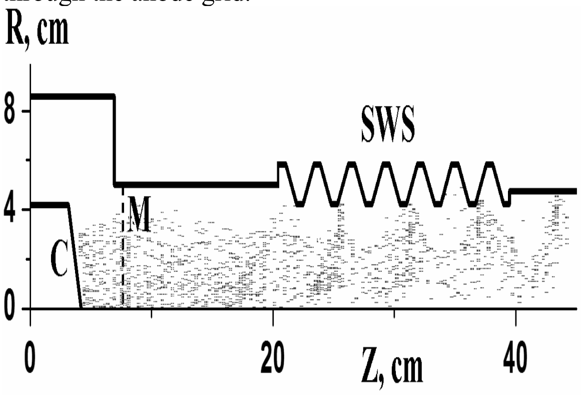

Fig. 3. Design of the oscillator.

With the code KARAT, we have calculated the regime of oscillation with a power efficiency of ≈ 30% on the operating E_{01} mode for a near-experimental shape of the voltage pulse at the cathode in the absence of an external magnetic field. For the stationary stage (t ≈ 35—50 ns), the calculated power was 3.1 GW at a frequency of 3.95 GHz (Fig. 4).

The electrodynamic characteristics of the simulated oscillator geometry at the operating frequency were studied with a program based on the scattering matrix method [9]. The calculations have shown that in the SWS section the phase velocity of the traveling wave E_{01} approximates c. The form of the "cold" longitudinal distribution of the field indicates that a standing wave occurs in the region between the grid and the SWS entrance where efficient energy modulation of the electron beam is likely to proceed.

For the longitudinal distribution of the z-component of the high-frequency electric field, between the anode grid and the SWS output, the assessed value of the active component of the electron flow susceptibility with $V_{e,0} \approx 0.95c$ is positive. The cold Q-factor of the operating oscillation was ≈ 30. Analysis of the dispersion characteristic of the operating wave E_{01} for the SWS section which has been obtained in the approximation of an infinite corrugated waveguide shows that the working point is near the calculated oscillation frequency.

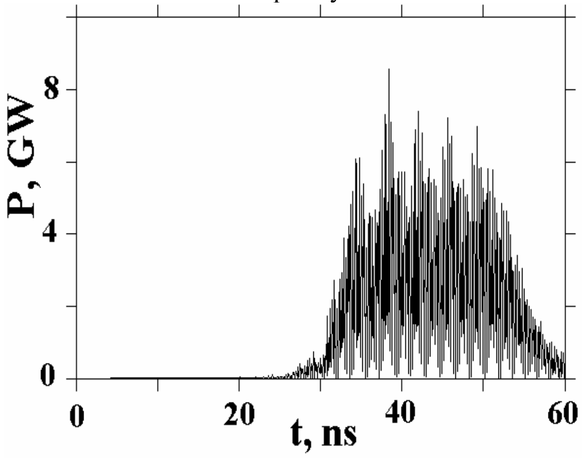

Fig. 4. Simulated time unaveraged output power flux. The parameters of the electron beam: electron energy 1.1 MeV, beam current 8.8 kA. The oscillation frequency: 3.95 GHz.

4. Experimental results

The proposed oscillator circuit has been tested experimentally on the nanosecond electron acceleratore SINUS-7 [10] which produced an electron beam with a peak current of ≈ 13 kA and a duration of ~50 ns in a planar diode in the single-pulse mode at a peak diode voltage of ≈ 1.3 MV. The anode grid was made of stainless steel wire of diameter 0.2 mm. Electrons were emitted from a metal-dielectric multi-blade cathode placed inside a focusing stainless steel electrode. The oscillation power was determined using a calibrated waveguide-to-strip line coupler and also through integration of the power flux density over the radiation pattern. Before integrating, the power flux density was measured with a short electric dipole at a distance of ≈ 4 m from the window of the radiating horn.

The radiation spectrum was determined through processing the radio signal fixed by an oscilloscope TDS-6604 using fast Fourier transform. For visual observation of the radiation pattern, use was made of a panel with neon-filled lamps.

With the optimal gap between the anode grid and the cathode, a mode with a power efficiency of 8±2 % was realized (Fig. 5). The peak power measured using the waveguide-to-strip line coupler and integration over the radiation pattern was 1.2±0.3 GW at a frequency of 4.06 GHz. The radiation pattern corresponded to the E_{01} wave. At a level of – 3 dB, the spectrum width was not larger than 100 MHz. In this mode, the maximum spread of microwave signal amplitudes was no greater than 25 %. Tuning out from the optimal gap causes a decrease in efficiency and an increase in power spread from pulse to pulse.

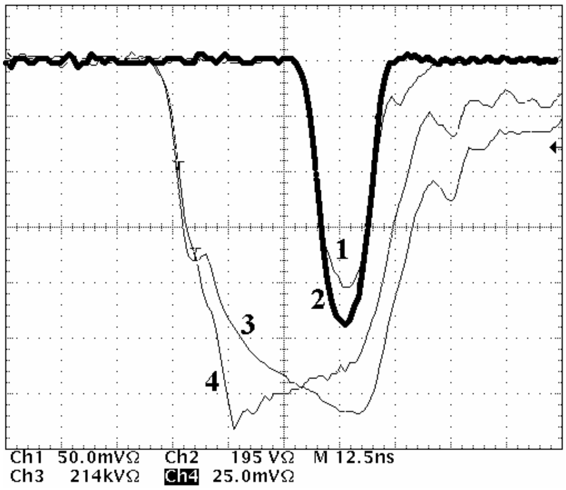

Fig. 5. Detected microwave signal from the waveguide-to-strip line coupler (1) and antenna (2), diode current with a peak value of ≈ 13 kA (3), and diode voltage with a peak value of ≈ 1.3 MV (4).

5. Conclusion

The large difference observed between the calculated and measured efficiency of the oscillator can be associated in part with specific formation of a continuous electron beam in the region of a planar vacuum diode. For instance, a large role can be played by parasitic electron flows from the focusing electrode (the transmitted current measured immediately behind of the anode grid was ≈ 60% of the total current), peculiarities of the formation and operation of emission centers at the edges of the cathode blades, not optimal profile of the cathode surface and nonuniformity of the electric field distribution near the anode grid with finite mesh size. The foregoing peculiarities are likely to affect the quality of the electron beam (e.g., spread of longitudinal velocities), its configuration in the region downstream of the anode grid (path length), and are characteristic of the experiment with a vircator [1]. On the other hand, it is not improbable that the experimental geometry of the SWS requires some additional optimization.

Thus, in the experiment the oscillation mode of the relativistic Cherenkov oscillator without external magnetic field has been realized with an efficiency of ≈ 8 % and with selective excitation of the E_{01} mode at a frequency close to the calculated one.

This work was partly supported by Russian Foundation for Basic Research (project No 05-02-08028).

References

[1] S.A. Kitsanov, A.I. Klimov, S.D. Korovin, et. al., Zhur. Tekh. Fiz., V. 72, No. 5, pp. 82-90 (2002).

[2] M. D. Haworth, G. Baca, James N. Benford, et al., IEEE Trans. Plasma. Sci. Vol. 26. No. 3. June 1998. P. 312-319.

[3] N.F. Kovalev, M.I. Petelin, M.D. Raizer, et. al., in book: *Relativistic high-frequency electronics,* Institute of Applied Physics, AS, USSR, Gorky, 1979, p. 76-113.

[4] L.D. Landau, E.M. Livshits, *Electrodynamics of solid media,* Fizmatlit, Moscow, 1959

[5] Tarakanov V. P. *User's Manual for Code KARAT.* Springfield: BRA, 1992

[6] S.D. Korovin, I.K. Kurkan, V.V. Rostov, et. al., Izv. Vyssh. Ucheb. Zaved., Radiofiz., 1999, V.42, No. 12., p. 1189-1196.

[7] V.L. Bratman, N.S. Ginzburg, N.F. Kovalev, et al., in book.: *Relativistic high-frequency electronics,* Institue of Applied Physics, AS, USSR, Gorky, 1979, p. 249-274.

[8] V.K. Yulpatov, Izv. Vyssh. Ucheb. Zaved. Radiofiz., 1970, V. 13, No. 12, p. 1784-1788.

[9] Denisov G.G, Lukovnikov D.A., Samsonov S.V., Int. J. Infrared and Millimeter Waves, 1995, V. 16, No. 4, p. 745-752.

[10] S.D. Korovin, V.V. Rostov, Izv. Vyssh. Ucheb. Zaved. Fiz., 1996, No. 12, p. 21-30.